Scilight

Nano-electrochemistry & Nano-photochemistry

https://www.sciltp.com/journals/nenp

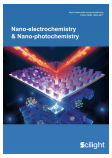

Article

Check for updates

Portable Colorimetric Sensor Based on DNA-Ag/Pt Bimetallic Nanozyme Sensing Kit for Quantitative Detection of *Staphylococcus aureus*

Wen Qiu, Yiwei Wang, Shan Huang * and Xiaojun Chen *

College of Chemistry and Molecular Engineering, Jiangsu Provincial University Key Laboratory of Intelligent Medical Sensing Materials and Devices, State Key Laboratory of Materials-Oriented Chemical Engineering, Nanjing Tech University, 30 South Puzhu Road, Nanjing 211816, China

* Correspondence: huangshan@njtech.edu.cn (S.H.); chenxj@njtech.edu.cn (X.C.)

How To Cite: Qiu, W.; Wang, Y.; Huang, S.; et al. Portable Colorimetric Sensor Based on DNA-Ag/Pt Bimetallic Nanozyme Sensing Kit for Quantitative Detection of *Staphylococcus aureus*. *Nano-electrochemistry & Nano-photochemistry* **2026**, *2*(2), 9. https://doi.org/10.53941/nenp.2026.100009

Received: 10 March 2026
Revised: 1 May 2026
Accepted: 6 May 2026
Published: 11 May 2026

Abstract: Utilizing the high specificity of nucleic acid aptamers toward *Staphylococcus aureus* (*S. aureus*) and the peroxidase-like activity of Ag/Pt nanoclusters (Ag/Pt NCs), this study developed a portable "DNA-nanozyme" sensing kit for rapid and quantitative bacterial detection. In this strategy, *S. aureus* was first captured by biotinylated aptamers immobilized on a streptavidin-coated microplate and then further recognized by aptamer-functionalized Ag/Pt NCs (DNA-Ag/Pt NCs), forming a sandwich-type sensing interface. The localized nanozyme probes efficiently catalyzed the chromogenic reaction of 3,3′,5,5′-tetramethylbenzidine (TMB) in the presence of hydrogen peroxide (H_2O_2), enabling both visual readout and quantitative absorbance analysis. The assay exhibits a linear dynamic range from 10^1 to 10^6 CFU mL^{-1}, with a limit of detection as low as 2.4 CFU mL^{-1}, and shows negligible cross-reactivity with non-target bacterial strains. This platform provides a robust and field-deployable tool for point-of-care bacterial detection and on-site food safety screening.

Keywords: *Staphylococcus aureus*; Ag/Pt nanoclusters; colorimetric detection; aptamer; point-of-care testing

1. Introduction

The high incidence, broad affected population, and potential severity of foodborne diseases have long been a primary concern in global public health, imposing substantial medical and socioeconomic burdens [1,2]. According to assessments by the World Health Organization (WHO) and related research, the burden of foodborne diseases is closely associated with biological hazards such as bacteria, viruses, and parasites, with particularly significant impacts observed in low- and middle-income countries [3]. Among the myriad of foodborne bacterial pathogens, *S. aureus*, a prototypical gram-positive bacterium, can be detected in milk, dairy products, and their associated processing environments, thereby presenting a persistent contamination risk [4,5]. Its pathogenicity primarily arises from various enterotoxins (exhibiting certain thermal stability) and virulence factors, including hemolysin and leukocidin. Consumers ingesting contaminated food may develop acute gastroenteritis within a short timeframe; in severe cases, the infection can escalate to invasive disease, resulting in more critical clinical outcomes [6,7]. Consequently, the development of a rapid, real-time, and field-applicable detection method for *S. aureus* holds significant importance for food safety surveillance, early epidemic alerting, and public health protection.

Currently, conventional pathogen detection methods predominantly rely on plate culture, quantitative real-time polymerase chain reaction (qPCR), and enzyme-linked immunosorbent assay (ELISA) [8]. Although plate culture yields reliable results, it typically necessitates a cultivation and confirmation period ranging from 24 h to

72 h or even longer, coupled with stringent operational procedures and laboratory conditions, thereby constraining its suitability for on-site emergency screening. QPCR exhibits high sensitivity and specificity, nevertheless, it is contingent upon thermal cycling and fluorescence detection instrumentation. Furthermore, the sample pre-treatment and detection design are relatively intricate, rendering the workflow more vulnerable to deviations in operating standards, data quality control, and contamination management [9]. ELISA technology is well-established, yet it often entails multiple incubation and washing steps. To enhance portability, paper-based or microfluidic ELISA variants have been investigated, however, in complex food matrices, non-specific adsorption and background signals may still compromise their performance [10]. In light of these limitations, concerted efforts have been directed towards developing simpler, more rapid, and more readily integrable methods, thereby diminishing the reliance on instruments while preserving specificity [11].

Nucleic acid aptamers, obtained via systematic evolution of ligands by exponential enrichment (SELEX), can fold into defined three-dimensional conformations and bind targets with high affinity. Their amenability to chemical synthesis and modification, together with favorable batch-to-batch consistency, makes them attractive recognition elements in biosensing applications [12]. In pathogen detection, aptamers can be readily integrated with magnetic carriers, paper-based platforms, or nanomaterials, facilitating modular integration of recognition, enrichment, and signal readout to simplify on-site operation [13–15]. For signal amplification, nanozymes, owing to their stability and tunability provide enzyme-mimicking catalytic functions and are widely used to amplify signals in colorimetric, fluorescent, or electrochemical readouts, thereby promoting point-of-care testing (POCT) device development [16,17]. Recent progress has further broadened the design of nanozyme-based sensing systems through controllable catalytic reactions and adaptable signal readout strategies [18–20]. In particular, bimetallic nanozymes often exhibit enhanced peroxidase-like activity through compositional synergism, enabling efficient catalysis of H_2O_2-mediated oxidation of TMB and thereby supporting high-contrast visual readouts [21]. Moreover, metal nanocluster mediated amplification can be combined with magnetic separation and multiplex encoding strategies to enable more flexible analytical schemes and multi-analyte detections [22–24]. With the widespread availability of portable terminals and algorithmic processing, smartphone-based image acquisition and quantitative analysis have also been employed to improve the standardization of on-site readouts and to advance the visualization and quantification of detection platforms [25–28].

On this basis, we propose a Point-of-Care Testing (POCT) kit for detecting *S. aureus* (Scheme 1). We employed a comprehensive strand reduction method to synthesize DNA-Ag/Pt bimetallic nanozymes (DNA-Ag/Pt NCs), incorporating sequences of *S. aureus* Apt and the synthesized Ag/Pt NCs. These nanozymes exhibit both high catalytic activity and excellent selectivity towards *S. aureus*, rendering them robust probes for constructing POCT kits. Initially, we immobilized biotinylated aptamers (Bio-Apt) onto a 96-well plate modified with streptavidin at the bottom. When the test sample was co-incubated with the DNA-Ag/Pt NCs, the Apt on the Ag/Pt NCs nanozyme specifically recognized *S. aureus* in the sample. Subsequently, after introducing the mixture containing *S. aureus* and DNA-Ag/Pt NCs into the kit, it was specifically captured by the Bio-Apt attached to the plate bottom. Following washing and purification steps, the catalytic system TMB-H_2O_2 was added to facilitate the visual detection of the kit. To further amplify the detection signal for intuitive readout, we utilized ImageJ software to digitize the detection signal, enabling on-site, highly sensitive and quantitative detection of *S. aureus* without reliance on large instruments.

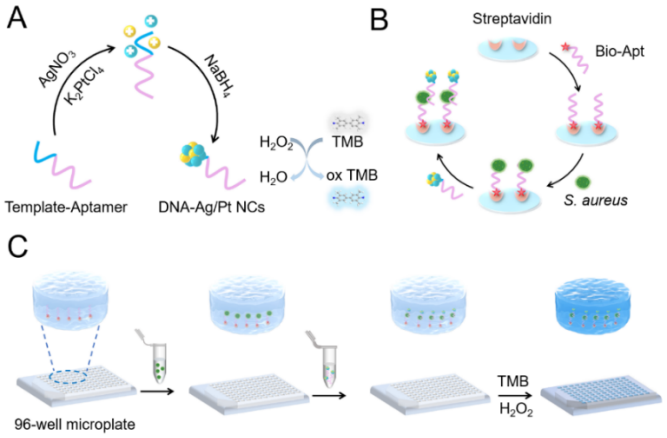

Scheme 1. Schematic diagram of the DNA-nanozyme sensing kit for ultrasensitive quantitative detection of *S. aureus*. (**A**) Schematic diagram of the synthesis process of DNA-Ag/Pt NCs. (**B**) Modification and connection of the bottom of 96-well plate. (**C**) The detection process of the DNA-nanozyme sensing kit.

2. Materials and Methods

2.1. Reagents and DNA Sequences

All oligonucleotides used in this study were synthesized by Sangon Biotech Co., Ltd. (Shanghai, China) and purified by HPLC. The sequences were summarized in Table 1.

Table 1. Sequences of the used oligonucleotides.

Name	Sequence (5′-3′)
Template	CCCCCTAACTCCCCC
S. aureus Apt	ATCCAGACGTGACGCAGCATGCGGTTGGTTGCGGTTGGGCATGATGTATTTCTGTGTGGAC ACGGTGGCTTAGTA
Bio-Apt	Bio- ATCCAGACGTGACGCAGCATGCGGTTGGTTGCGGTTGGGCATGATGTATTTCTGTGTGGAC ACGGTGGCTTAGTA
Template-Apt	CCCCCTAACTCCCCCATCCAGACGTGACGCAGCATGCGGTTGGTTGCGGTTGGGCATGATG TATTTCTGTGTGGACACGGTGGCTTAGTA

Silver nitrate ($AgNO_3$), sodium borohydride ($NaBH_4$), and H_2O_2 were purchased from Sinopharm Chemical Reagent Co., Ltd. (Shanghai, China). Potassium tetrachloroplatinate (II) (K_2PtCl_4) was obtained from J&K Scientific Ltd. Chloroauric acid tetrahydrate ($HAuCl_4 \cdot 4H_2O$), trisodium citrate dihydrate ($C_6H_5Na_3O_7 \cdot 2H_2O$) and PBS buffer were purchased from Nanjing Wanqing Glassware & Chemical Instrument Co., Ltd. Bovine serum albumin (BSA), TMB, tris(2-carboxyethyl)phosphine hydrochloride (TCEP), Tween-20, 4S GelBlue nucleic acid stain (10,000×aqueous solution), 50×TAE buffer, 5×TBE buffer, 40% acrylamide/bisacrylamide solution (37.5:1), N,N,N′,N′-tetramethylethylenediamine (TEMED), DNA molecular weight marker A (25–500 bp), and DNA loading buffer were purchased from Sangon Biotech Co., Ltd. (Shanghai, China). Streptavidin-coated 96-well plates were obtained from Nanjing Hooke Biotechnology Co., Ltd. All solutions were prepared with ultrapure water from a Milli-Q system (18 MΩ·cm). Unless otherwise specified, all reagents were of analytical grade.

2.2. Instrumentation

Polyacrylamide gel electrophoresis (PAGE) was performed using a Tanon MINI SPACE 1000 imaging system (Shanghai Tianneng Technology Co.). Transmission electron microscopy (TEM) images were recorded using a Talos L120C microscope. UV-vis absorption spectra were measured with a UV-vis spectrophotometer (LAMBDA 950). Zeta potential and dynamic light scattering (DLS) measurements were carried out using a laser particle size analyzer (90PlusPALS). Fluorescence measurements were performed on a fluorescence spectrophotometer (F97Pro, China).

2.3. Synthesis of DNA-Ag/Pt NCs

In 10 mM phosphate buffer (pH 7.0), $AgNO_3$ (150 μM, 5 μL) and K_2PtCl_4 (125 μM, 12 μL) were sequentially added to a template DNA solution (2 μM, 30 μL). After incubation in the dark at 4 °C for 30 min, freshly prepared $NaBH_4$ (5 mM, 3 μL) was rapidly injected to initiate the reduction reaction. The mixture was vigorously vortexed and then shaken at 37 °C for 3 h to obtain DNA-Ag/Pt NCs.

2.4. Synthesis of AuNPs

Gold nanoparticles (AuNPs) with an average diameter of approximately 15 nm were synthesized via the classical sodium citrate reduction method. Briefly, 3.4 mL of 1% $HAuCl_4$ solution was added to 96.6 mL of ultrapure water and heated to boiling under vigorous stirring. Subsequently, 10 mL of 38.8 mM trisodium citrate dihydrate solution was rapidly injected into the boiling solution. As the reaction proceeded, the solution color gradually changed from pale yellow to wine red, indicating the formation of AuNPs. The mixture was maintained under boiling and stirring for 15 min, followed by an additional 15 min of stirring after removal of the heat source, and then allowed to cool naturally to room temperature for further use.

2.5. Preparation of Apt-AuNPs

To prepare aptamer-functionalized AuNPs (Apt-AuNPs), 15 μL of 100 μM thiol-modified aptamer solution was mixed with 1.5 μL of 100 mM TCEP and incubated at room temperature for 1 h to reduce the terminal disulfide bonds and activate the thiol groups. The activated aptamer was then added to 500 μL of AuNPs solution and incubated at room temperature for 16 h, allowing immobilization of the aptamer onto the AuNP surface through

Au-S bonding. Thereafter, 50 μL of 1 M NaCl was added to adjust the final salt concentration to 0.1 M, and the mixture was further incubated at room temperature for 24 h to improve the stability of aptamer functionalization. After the reaction, the suspension was centrifuged at 12,000 rpm for 30 min to remove excess unbound aptamer. The resulting pellet was redispersed in ultrapure water and stored at 4 °C for subsequent use.

2.6. Peroxidase-like Activity of DNA-Ag/Pt NCs

The peroxidase-like activity of DNA-Ag/Pt NCs was evaluated by their catalysis of H_2O_2-mediated oxidation of TMB in acetate buffer. In a typical experiment, DNA-Ag/Pt NCs (50 μL, 2 μM), H_2O_2 (20 μL, 80 mM), and TMB (20 μL, 0.4 mM) were added to 110 μL of HAc-NaOAc buffer (0.2 M, pH 4.0). The reaction proceeded at room temperature for 10 min, after which the absorbance at 652 nm was recorded using a UV-vis spectrophotometer.

2.7. Specificity Verification of the Aptamer for S. aureus

Frozen *S. aureus* stocks were inoculated into a 15 mL round-bottom centrifuge tube containing 5 mL of LB medium and revived overnight at 37 °C with shaking at 120 rpm. After measurement of OD_{600}, 1 mL of the bacterial suspension was collected and centrifuged at 4 °C and 4000 rpm for 10 min. The supernatant was discarded, and the pellet was resuspended in sterile PBS buffer. This washing step was repeated three times. Subsequently, 20 μL of Apt-AuNPs with an average diameter of approximately 15 nm was added separately to suspensions of *S. aureus*, *Bacillus subtilis* (*B. subt*), *Staphylococcus epidermidis* (*S. epider*), and *Escherichia coli* (*E. coli*), followed by incubation at room temperature for 30 min. The mixtures were then centrifuged at 4 °C and 4000 rpm for 20 min. By visual inspection, the *S. aureus* sample produced the largest pellet area and the darkest color, indicating the strongest specific binding and aggregation between the Apt-AuNPs probe and the target bacterium. In contrast, the pellets formed with the other three non-target bacteria were markedly smaller and lighter in color, providing strong evidence that the aptamer selected in this study exhibits high specificity toward *S. aureus*. After imaging, all photographs were uniformly cropped and adjusted for brightness and contrast, and quantitative analysis was performed using ImageJ. The red sediment region was defined while excluding interference from isolated red lines, and the relative color-development area was calculated to evaluate recognition efficiency.

2.8. Preparation and Analysis of 12% PAGE

A 12% polyacrylamide gel was prepared by mixing 4 mL of distilled water, 1.6 mL of 5 × TBE buffer, 2.4 mL of 40% acrylamide/bisacrylamide solution, 56 μL of 10% APS, and 8 μL of TEMED in a dry beaker under continuous stirring. The resulting solution was then poured into the gel-casting plate and allowed to polymerize for 45 min at room temperature.

For PAGE analysis, different DNA samples were mixed with 6×DNA loading buffer at a volume ratio of 5:1 and gently vortexed. Then, 10 μL of each sample was loaded into individual gel lanes. Electrophoresis was carried out on the freshly prepared 12% gel using 1 × TBE buffer (pH 8.0) as the running buffer at 150 V for 45 min at room temperature. After electrophoresis, the gel was stained with GelRed for 10 min and subsequently imaged.

2.9. Construction of the Portable DNA-Ag/Pt NCs Sensing Kit

The procedure was as follows. Briefly, 100 μL of 100 nM biotinylated DNA aptamer was added to the streptavidin-coated plate and incubated at 37 °C for 1 h, allowing the aptamer to be immobilized on the bottom of the well through the streptavidin-biotin interaction. The wells were then blocked with 100 μL of BSA solution at 37 °C for 30 min to reduce nonspecific adsorption of the target on the plate surface. After each step, the wells were washed with sterile PBS buffer. Subsequently, 100 μL of *S. aureus* samples at different concentrations was added to each well and incubated for 2 h. After removal of the solution, 50 μL of DNA-Ag/Pt NCs was added. The specific DNA aptamers modified on the surface of the Ag/Pt NCs further bound to *S. aureus* and the mixture was incubated at 37 °C for another 2 h. After three washing steps to remove the unbound components, TMB and H_2O_2 were added for the colorimetric reaction, thereby enabling highly sensitive detection of *S. aureus*.

2.10. Bacterial Culture

LB medium was used for bacterial culture. After sterilization at 121 °C for 20 min and cooling to room temperature, *S. aureus*, *B. subt*, *S. epider*, *E. coli* and *Enterobacter aerogenes* (*E. aero*) were inoculated and shaken at 100 rpm in LB medium at 37 °C for 18 h. The enriched bacterial cells were collected by centrifugation

at 8000 rpm for 5 min and washed once with PBS. The harvested bacteria were resuspended in sterile PBS buffer (10 mM, pH 7.4) and diluted to the required concentrations for subsequent use.

2.11. Analysis in Real Samples

Milk, beef, and drinking water were selected as representative real samples to evaluate the practical applicability of the proposed sensing kit. Milk samples were diluted ten-fold with sterile PBS buffer before analysis. Beef samples were first minced into small pieces to facilitate subsequent homogenization. Then, 1.0 g of minced beef was mixed with 9.0 mL of sterile PBS buffer and homogenized thoroughly to obtain a uniform suspension. The homogenate was centrifuged at 8000 rpm for 5 min to remove large tissue residues, and the supernatant was further filtered through a 0.22 μm microfiltration membrane to remove residual tissue debris and insoluble impurities. The obtained filtrate was used as the beef sample matrix for subsequent analysis. Drinking water samples were directly used without additional pretreatment. For recovery tests, *S. aureus* was spiked into the prepared milk, beef homogenate, and drinking water samples at final concentrations of 10^1, 10^2, and 10^3 CFU/mL, followed by detection using the DNA-Ag/Pt NCs sensing kit under the optimized conditions. In addition, milk and beef samples stored overnight were analyzed using the same procedure. Recovery and relative standard deviation (RSD) values were calculated based on parallel measurements.

3. Results and Discussion

3.1. Synthesis and Characterization of DNA-Ag/Pt NCs

The preparation of high-performance signal probes is crucial for this sensing system. We synthesized DNA-Ag/Pt NCs using an optimized "one-pot" method, which is simple, efficient, and effectively controls the size and stability of the NCs through the DNA template. In this process, DNA was not only used as a stabilizing matrix, but also participated in the controlled formation of Ag/Pt NCs. The C-rich segment in the DNA template could interact with Ag^+, helping localize Ag^+ along the DNA strand before reduction. After $NaBH_4$ reduction, the formed Ag NCs further promoted Pt deposition and growth, leading to the formation of Ag/Pt NCs. The DNA matrix helped restrict excessive metal growth and random aggregation, thereby contributing to the nanoscale size, good dispersion, and colloidal stability of the Ag/Pt NCs. More importantly, the Template-Apt sequence combined the nanocluster-forming domain with the *S. aureus* Apt sequence. Thus, the same DNA strand linked nanocluster construction, target recognition, and catalytic signal output, which was essential for building the subsequent DNA-Ag/Pt NCs-based sensing kit. The transmission electron microscopy (TEM) image in Figure 1A shows that the as-prepared DNA-Ag/Pt NCs exhibit a generally spherical morphology, with most particles distributed in the range of approximately 4–10 nm and good dispersibility. Their nanoscale size is attributed to the stabilizing effect provided by the DNA template. The dynamic light scattering (DLS) profile further indicates that the hydrodynamic diameter of the DNA-Ag/Pt NCs is about 7 nm, consisting with the particle size distribution results measured by TEM. The energy dispersive X-ray (EDX) spectrum displays distinct signals for Ag and Pt, confirming the successful construction of the bimetallic NCs (Figure 1B). Fluorescence spectroscopy reveals that, compared to the brightly emissive DNA-Ag NCs, the fluorescence of DNA-Ag/Pt NCs is almost completely quenched, indicating the successful deposition of Pt NCs on the surface of Ag NCs (Figure 1C). UV-vis spectroscopy shows a characteristic DNA absorption peak at 260 nm, confirming the successful modification of DNA on the Ag/Pt NCs (Figure S1). Evaluation of catalytic performance demonstrates that after introducing DNA-Ag/Pt NCs into the TMB-H_2O_2 system and reacting for 10 min, the absorbance at 652 nm reaches about 0.8, corresponding to the characteristic peak of the oxidized TMB, indicating the peroxidase-like activity of the material (Figure 1D). In contrast, DNA-Ag NCs exhibit almost no catalytic response, further highlighting the critical role of Ag/Pt bimetallic NCs in catalysis. It should be noted that the catalytic activity test in Figure 1D was different from the subsequent biosensing assay in experimental format. This catalytic performance test was conducted in a free-solution system, where DNA-Ag/Pt NCs were directly mixed with TMB and H_2O_2 at a relatively sufficient probe concentration. Therefore, the absorbance value mainly reflects the intrinsic peroxidase-like activity of dispersed DNA-Ag/Pt NCs. However, the final signal was generated only by the DNA-Ag/Pt NCs captured on the microplate through the Apt-mediated sandwich structure in the biosensing assay, while unbound probes were removed during the washing steps. As a result, the effective amount of DNA-Ag/Pt NCs participating in the chromogenic reaction was much lower than that in the catalytic activity test, leading to a relatively lower absorbance at 652 nm. Thus, the difference in absorbance mainly arises from

the different assay formats, probe amounts, and washing procedures rather than inconsistent catalytic behavior.

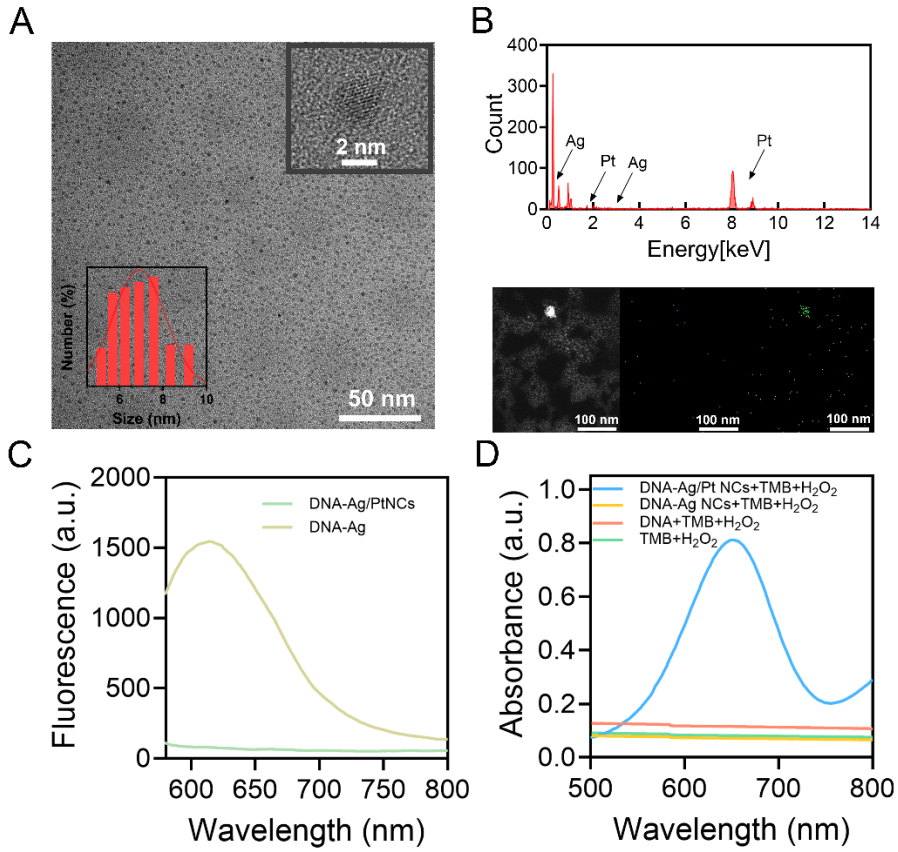

Figure 1. Morphology and property characterization of DNA-Ag/Pt NCs. (**A**) TEM image of DNA-Ag/Pt NCs. Inset: High-resolution TEM image and the particle size distribution histogram of DNA-Ag/Pt NCs; (**B**) EDX spectrum of DNA-Ag/Pt NCs; (**C**) Fluorescence emission spectra of DNA-Ag NCs and DNA-Ag/Pt NCs under laser irradiation at 548 nm; (**D**) UV-vis absorption spectra of different samples.

3.2. Specificity Verification of Aptamer Recognition and Feasibility of the Sensing Kit

Figure 2A demonstrates the specificity of the selected Apt for the detection of *S. aureus*. In this study, a colorimetric detection method based on Apt-modified AuNPs was employed for validation. This method offers rapid response, reliable results, and potential for on-site application. In the experiment, 15 nm AuNPs served as colorimetric probes, and thiol-modified Apt were immobilized on their surface via stable Au-S bond to form Apt-AuNPs conjugates. After incubating the conjugates with different bacterial species and subsequent centrifugation, distinct color differences in the pellets were visually observable. In the photo of Figure 2A, from left to right, the conjugation performance of *S. aureus*, *B. subt*, *S. epider*, and *E. coli* with Apt-AuNPs was exhibited, respectively. It could be found that only the pellet corresponding to *S. aureus* displayed the largest area and the darkest color, confirming the high specificity of the Apt toward the target bacterium. This experiment was designed to examine the binding ability of the Apt itself rather than the signal output of AuNPs. In the Apt-AuNPs system, AuNPs mainly acted as visible carriers to show the interaction between the Apt and bacteria. Since the same *S. aureus* Apt was introduced onto DNA-Ag/Pt NCs in the following sensing system, the selective binding behavior observed here provides direct support for the recognition function of the DNA-Ag/Pt NCs probes. Therefore, the specificity verified by the Apt-AuNPs assay could be reasonably extended to the DNA-Ag/Pt NCs-based sensing kit. Figure 2B further verifies the feasibility of the constructed DNA-nanozyme sensing kit for detecting *S. aureus*. In the TMB-H_2O_2 chromogenic system, a significant increase in absorbance at 652 nm was observed only when *S. aureus* was present together with DNA-Ag/Pt NCs, indicating successful nanozyme-catalyzed color development. In contrast, all other control groups showed absorbance levels close to the baseline, with no apparent colorimetric response. These results demonstrate that the proposed strategy can successfully establish a biosensor for the specific detection of *S. aureus*.

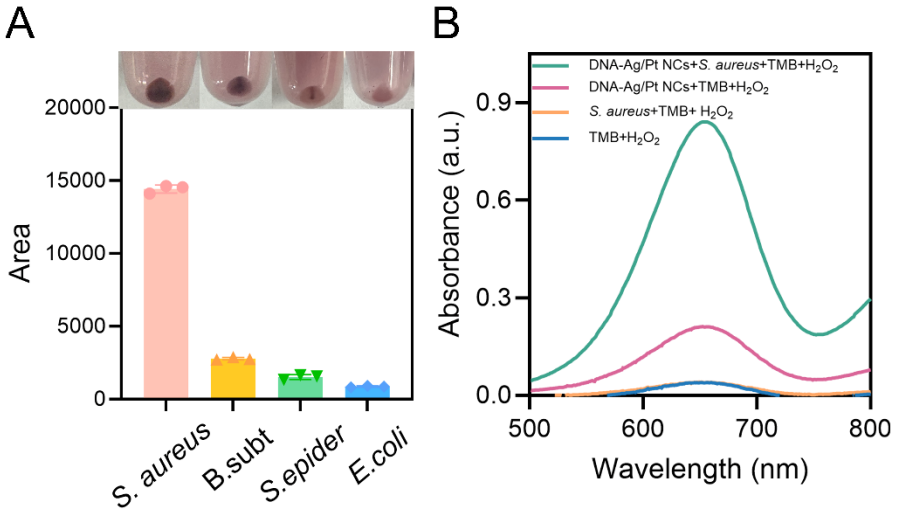

Figure 2. DNA-Ag/Pt NCs recognition specificity verification. (**A**) Image and statistical data chart demonstrating the recognition specificity of DNA-Ag/Pt NCs towards *S. aureus* by the AuNPs binding method. (**B**) UV-vis spectra at 652 nm for the DNA-nanozyme sensing kit in the presence of TMB-H_2O_2.

3.3. Optimization of the Sensing Conditions

Following the successful construction of the DNA-nanozyme sensing kit, the key reaction parameters were further optimized. The catalytic conditions of DNA-Ag/Pt NCs were first investigated in the absence of bacteria to determine a suitable TMB-H_2O_2 reaction system for the nanozyme probes. Considering that the introduction of bacteria may change the reaction microenvironment and affect the apparent absorbance response of the chromogenic system, the concentrations of H_2O_2 and TMB were subsequently re-evaluated in the presence of bacteria. This design allowed us to confirm whether the conditions optimized from the catalytic reaction alone could also be applied to the complete bacterial detection system. As shown in Figure S2, we first optimized the dosage ratio of K_2PtCl_4 vs. $AgNO_3$ in Ag/Pt NCs as 4:1 for the best catalytic performance. Subsequently, in the catalytic reaction system, we found that the Ag/Pt NCs exhibited the strongest activity in an acetate buffer at pH 4.0 (Figure S3A), with 80 mM H_2O_2 (Figure S3B) and 0.4 mM TMB (Figure S3C). Although 80 mM H_2O_2 is relatively high compared with some reported colorimetric assays, this concentration was chosen based on the optimized catalytic response of DNA-Ag/Pt NCs. Under this condition, the TMB oxidation reaction could generate a sufficient and stable absorbance signal within 10 min. Since H_2O_2 was added only in the final color-development step after bacterial capture and washing, it did not interfere with the aptamer-based recognition process, which supports the practical applicability of the assay. Based on this reaction system, we further monitored the catalytic kinetics and observed that the absorbance signal continuously increased and stabilized within 10 min (Figure S4). This systematic optimization ensures high sensitivity and reproducibility for subsequent detection, laying a solid foundation for constructing highly active signal probes. As shown in Figure 3A,B, the effects of different H_2O_2 and TMB concentrations on the absorbance at 652 nm were further evaluated in the presence of bacteria. The results showed that, within the investigated ranges, changes in H_2O_2 concentration did not lead to an obvious increase in absorbance, and a slight decrease was observed at higher concentrations. Meanwhile, variations in TMB concentration had only a minor effect on the absorbance. These results indicate that the introduction of bacteria did not significantly alter the response trend of the colorimetric system to substrate concentration. Taken together, 0.4 mM TMB and 80 mM H_2O_2 were selected as the final chromogenic conditions, as they provided a stable and sufficient absorbance response in both the nanozyme catalytic system and the complete bacterial sensing system. On this basis, the working parameters of each functional module of the kit were systematically optimized. We employed gel electrophoresis experiments to optimize the immobilization concentration of Bio-Apt at the bottom of the plate. When the concentration of Bio-Apt immobilized on the plate bottom reaches 200 nM, the specific binding between Bio-Apt and streptavidin modified on the kit bottom reaches saturation (residual DNA is present in the supernatant, lane 3), thereby establishing the optimal coating concentration for Bio-Apt (Figure S5). Further optimization of the blocking, capture, and signal amplification steps revealed that bacterial binding Apt reached equilibrium after 2 h of incubation (Figure 3C); blocking with bovine serum albumin (BSA) for 30 min effectively eliminated nonspecific adsorption (Figure 3D); and incubation with the DNA-Ag/Pt NCs probe for 2 h (Figure 3E) and a concentration of 2 μM (Figure 3F) achieved the maximum catalytic signal amplification efficiency. These parameters were determined as the optimal working conditions for the kit.

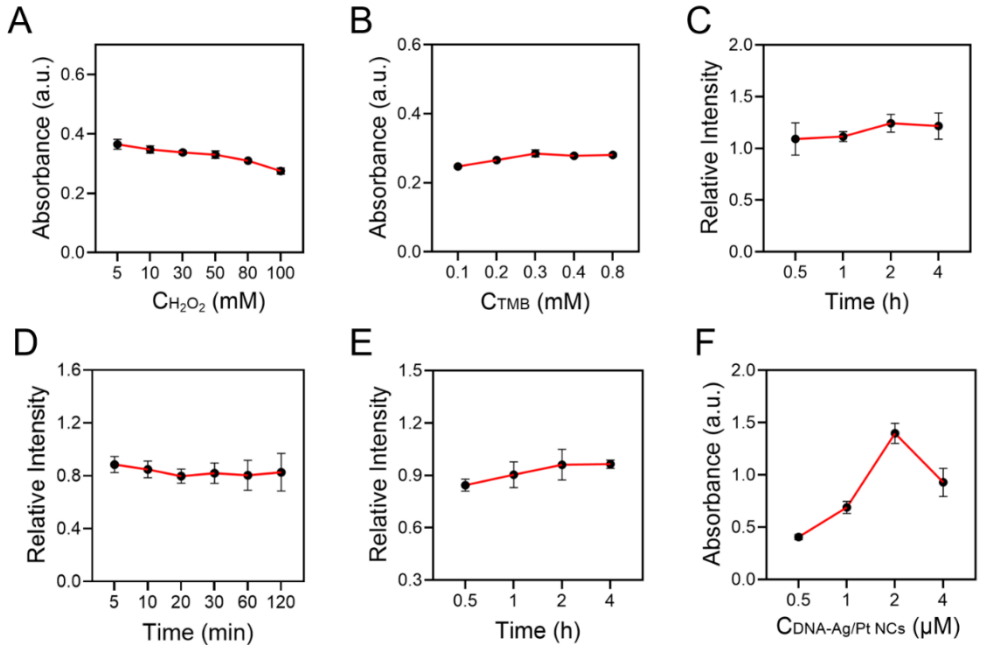

Figure 3. Optimization of key parameters for the sensing kit working system: (**A**) H_2O_2 concentration, (**B**) TMB concentration, (**C**) Bacterial incubation time, (**D**) BSA blocking time, (**E**) DNA-Ag/Pt NCs conjugation time, (**F**) DNA-Ag/Pt NCs concentration.

3.4. Sensitivity and Specificity of the DNA-Ag/Pt NC Sensing Kit for S. aureus Detection

To determine the limit of detection (LOD) of this method, a standard curve was constructed using *S. aureus* at seven concentrations ranging from 10^1 to 10^7 CFU/mL. As shown in Figure 4A, with increasing bacterial concentration, the system exhibited a visually discernible color gradient from light blue to dark blue, with distinct color differences. The absorbance at 652 nm showed an excellent linear relationship with the logarithm of bacterial concentration over the range of 10^1 to 10^6 CFU/mL, yielding a regression equation of $y = 0.0785x + 0.2188$ ($R^2 = 0.9903$) (Figure 4B). According to the LOD = 3σ/*S* calculation (where σ is the standard deviation of the negative control and *S* is the slope), the detection limit was evaluated as low as 2.4 CFU/mL.

After establishing the detection sensitivity, the specificity of the DNA-nanozyme sensing kit was further evaluated. Under identical experimental conditions, *S. aureus*, four potential interfering bacterial strains (*B. subt*, *E. aero*, *S. epider*, and *E. coli*), and a mixed bacterial sample were tested in parallel. For the single-bacterium groups, each bacterial suspension was adjusted to 10^6 CFU/mL before detection. In the mixed bacterial sample, *S. aureus*, *E. coli*, *E. aero*, *S. epider*, and *B. subt* were included, and the final concentration of each bacterial strain was also 10^6 CFU/mL. As shown in Figure 4C, the absorbance at 652 nm for the non-target bacterial groups was significantly lower than that for the *S. aureus* group. The mixed sample still produced an obvious absorbance response, although its signal was slightly lower than that of the single *S. aureus* group, indicating that the sensing kit could maintain good selectivity toward *S. aureus* in the presence of non-target bacteria.

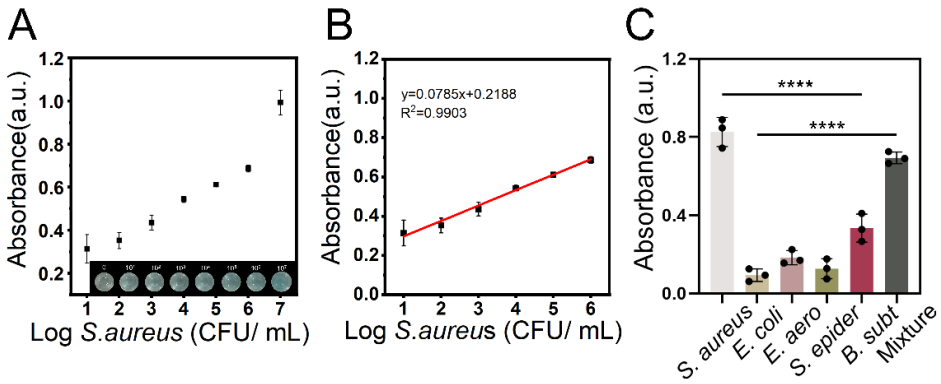

Figure 4. The sensitivity and specificity of DNA-Ag/Pt NCs sensing kit for *S. aureus* detection. (**A**) The absorbance of sensing kit with various concentrations of *S. aureus* from 10^1 to 10^7 CFU/mL. (**B**) The calibration curve for the detection of *S. aureus* based on the sensing kit. (**C**) The detection specificity of the sensing kit.

3.5. Detection in Real Samples

To assess the practical application potential of this method in real scenarios, spiked recovery experiments were conducted using three representative sample matrices, milk, beef homogenate, and drinking water. The known concentrations of *S. aureus* were introduced into the above samples, followed by detection using the proposed method to evaluate its accuracy and stability in complex sample environments. As shown in Table 2, for the spiked recovery experiments, the recoveries of *S. aureus* in milk, beef, and drinking water ranged from 94.1% to 112%, with RSD values of 2.2–6.9%. These results indicate that the proposed method can accurately detect *S. aureus* in different sample matrices with good repeatability. In addition, the applicability of the method was further evaluated using milk and beef samples stored overnight. The measured bacterial concentrations in the overnight milk and beef samples were 2.27×10^3 CFU/mL and 1.63×10^5 CFU/mL, respectively, with RSD values of 4.9% and 1.2%. Overall, these data fully validate the reliability and robustness of this sensing strategy for real sample detection, providing solid experimental evidence for its promotion and application in fields of food safety monitoring, clinical diagnostics, or environmental testing.

Table 2. Detection results of *S. aureus* in real food samples using the DNA-Ag/Pt NCs sensing kit.

Samples	Spiked (CFU/mL)	Measured (CFU/mL)	Recovery (%)	RSD (%)
Milk	10^1	0.989×10^1	98.9%	5.1%
	10^2	1.24×10^2	112%	4.7%
	10^3	0.941×10^3	94.1%	2.4%
Beef	10^1	1.07×10^1	107%	2.2%
	10^2	1.04×10^2	104%	3.4%
	10^3	0.967×10^3	96.7%	3.1%
Drinking water	10^1	0.978×10^1	97.8%	6.9%
	10^2	0.976×10^2	97.6%	3.7%
	10^3	1.03×10^3	103%	2.8%
Overnight milk		2.27×10^3		4.9%
Overnight beef		1.63×10^5		1.2%

4. Conclusions

This study successfully developed a detection kit based on an "Apt + nanozyme" coupling strategy for the rapid, highly sensitive, and specific detection of *S. aureus*. The core innovation of the kit lies in the use of DNA-Ag/Pt NCs synthesized via a one-pot method as signal tags, which exhibit excellent peroxidase-like activity and can efficiently catalyze the TMB-H_2O_2 chromogenic reaction, producing a strong blue signal visible to the naked eye and enabling quantitative absorbance measurement. The entire detection system establishes an integrated "recognition-detection" workflow. Target bacteria are captured by aptamers pre-immobilized on microplate wells, and a stable sandwich complex is formed through the specific binding of aptamers on the signal probes, thereby precisely localizing the nanozymes at the reaction interface and achieving efficient signal transduction and amplification. The method is simple to operate, rapid, and does not require sophisticated instruments, while also demonstrating outstanding sensitivity (LOD as low as 2.4 CFU/mL), high specificity, and good applicability to real samples. In summary, the sensing kit proposed in this study shows remarkable application potential and translational value in fields such as on-site rapid screening, primary healthcare diagnostics, food safety monitoring, and environmental pathogen surveillance, offering a powerful new tool for point-of-care detection of pathogenic bacteria.

Supplementary Materials

The additional data and information can be downloaded at: https://media.sciltp.com/articles/others/26051111 01083173/NENP-26040080-SI.pdf.

Author Contributions

W.Q.: methodology, software, data curation, writing—original draft preparation; Y.W.: data curation; S.H.: conceptualization, visualization, investigation, funding supporting, writing—reviewing and editing; X.C.: supervision, visualization, validation writing—reviewing and editing. All authors have read and agreed to the published version of the manuscript.

Funding

This work was supported by the National Key R&D Program Young Scientists Project of China (2024YFC3214300); the National Natural Science Foundation of China (no. 22304080); the Natural Science Foundation of Jiangsu Province (no. BK20230310); the Natural Science Foundation of the Jiangsu Higher Education Institutions of China (no. 23KJB150011).

Conflicts of Interest

The authors declare no conflict of interest. Given the role as journal editor, Xiaojun Chen had no involvement in the peer review of this paper and had no access to information regarding its peer-review process. Full responsibility for the editorial process of this paper was delegated to another editor of the journal. Shan Huang and Xiaojun Chen had involvement in conceptualization, visualization, investigation, writing—reviewing and editing. They take full responsibility for the content of the published article.

Use of AI and AI-Assisted Technologies

No AI tools were utilized for this paper.

References

1. Pires, S.M.; Desta, B.N.; Mughini-Gras, L.; et al. Burden of foodborne diseases: Think global, act local. *Curr. Opin. Food Sci*. **2021**, *39*, 152–159.
2. Grace, D. Burden of foodborne disease in low-income and middle-income countries and opportunities for scaling food safety interventions. *Food Secur*. **2023**, *15*, 1475–1488.
3. Keddy, K.H.; Hoffmann, S.; Founou, L.L.; et al. Quantifying national burdens of foodborne disease-Four imperatives for global impact. *PLOS Glob. Public Health* **2025**, *5*, e0004309.
4. Zhang, J.; Wang, J.; Jin, J.; et al. Prevalence, antibiotic resistance, and enterotoxin genes of *Staphylococcus aureus* isolated from milk and dairy products worldwide: A systematic review and meta-analysis. *Food Res. Int.* **2022**, *162*, 111969.
5. Li, X.; Zhang, J.; Zhang, H.; et al. Genomic analysis, antibiotic resistance, and virulence of *Staphylococcus aureus* from food and food outbreaks: A potential public concern. *Int. J. Food Microbiol*. **2022**, *377*, 109825.
6. Mairi, A.; Ibrahim, N.A.; Idres, T.; et al. A comprehensive review of detection methods for *Staphylococcus aureus* and its enterotoxins in food: From traditional to emerging technologies. *Toxins* **2025**, *17*, 319.
7. Di Bella, D.; Marini, B.; Stroffolini, G.; et al. The virulence toolkit of *Staphylococcus aureus*: A comprehensive review of toxin diversity, molecular mechanisms, and clinical implications. *Eur. J. Clin. Microbiol. Infect. Dis.* **2025**, *44*, 1797–1816.
8. Aladhadh, M. A review of modern methods for the detection of foodborne pathogens. *Microorganisms* **2023**, *11*, 1111.
9. Bustin, S.A. Improving the quality of quantitative polymerase chain reaction experiments: 15 years of MIQE. *Mol. Aspects Med.* **2024**, *96*, 101249.
10. Zhao, Y.N.; Zeng, D.X.; Yan, C.; et al. Rapid and accurate detection of *Escherichia coli* O157:H7 in beef using microfluidic wax-printed paper-based ELISA. *Analyst* **2020**, *145*, 3106–3115.
11. Guo, Y.Y.; Zheng, Y.; Liu, Y.J.; et al. A concise detection strategy of *Staphylococcus aureus* using N-succinyl-chitosan-doped bacteria-imprinted composite film and AIE fluorescence sensor. *J. Hazard. Mater*. **2022**, *423*, 126934.
12. Yoo, H.; Jo, H.; Oh, S.S. Detection and beyond: Challenges and advances in aptamer-based biosensors. *Mater. Adv*. **2020**, *1*, 2663–2687.
13. Zhang, H.W.; Yao, S.; Song, X.L.; et al. One-step colorimetric detection of *Staphylococcus aureus* based on target-induced shielding against the peroxidase mimicking activity of aptamer-functionalized gold-coated iron oxide nanocomposites. *Talanta* **2021**, *232*, 122448.
14. Gao, B.; Ding, Y.; Cai, Z.H.; et al. Dual-recognition colorimetric platform based on porous Au@Pt nanozymes for highly sensitive washing-free detection of *Staphylococcus aureus*. *Microchim. Acta* **2024**, *191*, 438.
15. Wei, S.N.; Li, J.; He, J.Y.; et al. Paper chip-based colorimetric assay for detection of *Salmonella typhimurium* by combining aptamer-modified Fe_3O_4@Ag nanoprobes and urease activity inhibition. *Microchim. Acta* **2020**, *187*, 554.
16. Wu, Y.Y.; Tian, X.; Jiang, Y.; et al. Advances in bimetallic materials and bimetallic oxide nanozymes: Synthesis, classification, catalytic mechanism and application in analytical chemistry. *TrAC Trends Anal. Chem*. **2024**, *176*, 117757.
17. Chi, Z.M.; Wang, Q.; Gu, J. Recent advances in colorimetric sensors based on nanozymes with peroxidase-like activity. *Analyst* **2023**, *148*, 487–506.
18. Gai, P.P.; Pu, L.; Wang, C.; et al. CeO_2@NC nanozyme with robust dephosphorylation ability of phosphotriester: A simple colorimetric assay for rapid and selective detection of paraoxon. *Biosens. Bioelectron*. **2023**, *220*, 114841.

19. Zhang, M.L.; Wang, Y.Q.; Li, N.; et al. Specific detection of fungicide thiophanate-methyl: A smartphone colorimetric sensor based on target-regulated oxidase-like activity of copper-doped carbon nanozyme. *Biosens. Bioelectron*. **2023**, *237*, 115554.
20. Zhu, D.Q.; Zhang, M.L.; Pu, L.; et al. Nitrogen-enriched conjugated polymer enabled metal-free carbon nanozymes with efficient oxidase-like activity. *Small* **2022**, *18*, 2104993.
21. Mu, X.M.; Li, J.S.; Xiao, S.X.; et al. Peroxidase-mimicking DNA-Ag/Pt nanoclusters mediated visual biosensor for CEA detection based on rolling circle amplification and CRISPR/Cas12a. *Sens. Actuators B* **2022**, *375*, 132870.
22. Wei, S.N.; Su, Z.Y.; Bu, X.G.; et al. On-site colorimetric detection of *Salmonella typhimurium*. *NPJ Sci. Food.* **2022**, *6*, 48.
23. Wei, S.N.; Wang, F.; Zhang, L.; et al. A portable smartphone-assisted highly emissive magnetic covalent organic framework-based fluorescence sensor for the detection of *Salmonella typhimurium*. *Sens. Actuators B* **2023**, *392*, 134076.
24. Su, Z.Y.; Wei, S.N.; Shi, X.N.; et al. Smartphone-assisted colorimetric detection of *Salmonella typhimurium* based on the catalytic reduction of 4-nitrophenol by β-cyclodextrin-capped gold nanoparticles. *Anal. Chim. Acta* **2023**, *1239*, 340672.
25. Wang, X.C.; Zhang, H.Q.; Li, H.; et al. A smartphone-enabled colorimetric platform based on enzyme cascade amplification strategy for detection of *Staphylococcus aureus* in milk. *J. Dairy Sci.* **2024**, *107*, 5438–5448.
26. Li, H.; Xu, H.; Yao, S.; et al. Target-inhibited MCOF-Apt-AuNPs self-assembly for multicolor colorimetric detection of *Salmonella Typhimurium*. *NPJ Sci. Food*. **2024**, *8*, 78.
27. Yao, S.; Pang, B.; Fu, Y.L.; et al. Multiplex detection of foodborne pathogens using inductively coupled plasma mass spectrometry, magnetic separation and metal nanoclusters-mediated signal amplification. *Sens. Actuators B* **2022**, *359*, 131581.
28. Shi, X.N.; Zhang, J.; Ding, Y.K.; et al. Ultrasensitive detection platform for *Staphylococcus aureus* based on DNAzyme tandem blocking CRISPR/Cas12a system. *Biosens. Bioelectron*. **2024**, *264*, 116671.